ORIGINAL RESEARCH ARTICLE

Research on the Leaching of Calcium Ions from De-vanadiumized Steel Slag for Indirect CO_2 Mineral Sequestration: Thermodynamics, Kinetics, and Parameter Optimization

RUNSHENG XU, YUCHEN ZHANG, JIANLIANG ZHANG, ANYANG ZHENG, MINGHUI CAO, and JIYONG YU

Steel slag is a kind of bulk alkaline industrial solid waste produced in the steelmaking process. Resource utilization of this solid waste is an urgent problem to be solved in the steel industry to achieve green and low-carbon development. Carbonation of steel slag is one of the key technologies for the utilization of steel slag and the reduction of CO_2 emission. It is also an important means to realize the green and low-carbon development of the steel industry. However, the low leaching efficiency of steel slag limits its industrial application. In order to obtain the best leaching conditions, the leaching behavior of de-vanadiumized steel slag in ammonium chloride was studied in this paper. The leaching rate model of calcium ions based on the minimum free energy was established by thermodynamic theory, and the leaching effect of calcium ions in ammonium chloride solution was evaluated, which was mutually confirmed with the single-factor experiment. Then, the response surface method was used to further study the effects of various factors and their interactions on the leaching rate, and a second-order polynomial model of the leaching rate was established. The results showed that the significance of the parameters affecting the leaching rate of calcium ions was steel slag particle size > liquid–solid ratio > leaching temperature > leaching time. After leaching steel slag particles with a size of 0.089 mm for 69.85 minutes at a liquid–solid ratio of 89.74 and a temperature of 80 °C, the calcium ion leaching rate reached a maximum of 49.76 pct. Based on the experimental data of single factor and response surface, the Drozdov equation with self-resistance coefficient and Arrhenius equation were used to establish a kinetic model to explore the restrictive link of leaching rate. The apparent activation energy of the reaction was calculated to be 20.428 kJ/mol, indicating that the leaching process was controlled by the liquid–solid interface chemical reaction and diffusion mixing. The research results of this paper further improve the theoretical basis of steel slag leaching of calcium ions and obtain more scientific leaching parameters, which can provide technical guidance for the industrialization and large-scale efficient production of carbon dioxide fixed by de-vanadiumized steel slag.

https://doi.org/10.1007/s11663-024-03000-w

I. INTRODUCTION

THE world's energy consumption has been steadily increasing over the years, resulting in a significant amount of greenhouse gas emissions, such as CO_2, CH_4, N_2O, *etc.*[1] Among them, the rise in atmospheric CO_2 concentration has the most substantial impact on global warming, causing extreme weather conditions and environmental disasters, such as floods, droughts, and sea level rise. According to the latest analysis report of the International Energy Agency, global CO_2 emissions

RUNSHENG XU and JIANLIANG ZHANG are with the State Key Laboratory of Advanced Metallurgy, University of Science and Technology Beijing, Beijing 100083, P.R. China and also with the School of Metallurgical and Ecological Engineering, University of Science and Technology Beijing, Beijing 100083, P.R. China. Contact e-mail: xurunsheng@ustb.edu.cn, zhang.jianliang@hotmail.com YUCHEN ZHANG is with the State Key Laboratory of Advanced Metallurgy, University of Science and Technology Beijing. ANYANG ZHENG, MINGHUI CAO and JIYONG YU are with the School of Metallurgical and Ecological Engineering, University of Science and Technology Beijing.

Manuscript submitted September 22, 2023; accepted January 5, 2024.

Article published online February 20, 2024.

are projected to reach 36.3 billion tons in 2021, resulting in an absolute increase of over 2 billion tons, which is the largest increase in history.[2] Consequently, there is an urgent need to reduce CO_2 emissions.

Carbon Capture, Utilization and Storage (CCUS) is one of the important options to curb the increase of CO_2 concentration in the atmosphere to mitigate climate change. Typical technologies are geological, marine, and fossil storage.[3,4] The first two methods mimic the natural storage of fossil fuels by injecting CO_2 into appropriate subsurface geological environments or the deep sea. Despite harboring immense potential for sequestration, these methods necessitate substantial resources for extended monitoring, introducing potential risks to both the environment and safety. These risks encompass geological damage, ecological harm, seismic activity, and the inadvertent leakage of CO_2.[5–7] In contrast, mineral storage mimics the natural weathering process of rocks by trapping CO_2 in the form of stable carbonates ($CaCO_3/MgCO_3$) permanently through the carbonation of calcium and magnesium components of various minerals (especially silicate minerals).[8] And because of its storage stability, production of high value products, and no need for later monitoring, CO_2 mineral storage emerges as a more promising candidate for industrial applications when compared to geological and marine storage alternatives.

The raw materials for CO_2 sequestration include natural minerals and industrial solid waste.[9–12] However, the exploitation of natural minerals is a process of high energy consumption and high pollution, which will have a negative impact on the environment again. Therefore, industrial solid waste is more suitable as a raw material for CO_2 capture. In addition, China has been the world's largest producer of steel for many years, with steel slag accounting for 15 to 20 pct of crude steel production.[13] Despite this, China's underutilization of steel slag results in environmental pollution and significant land occupation. Comprehensive utilization of steel slag not only mitigates its harmful effects but also transforms it into a valuable resource, yielding substantial economic benefits. On the other hand, steel slag is a basic slag, which has a relatively high reactivity compared to natural minerals and is more suitable for CO_2 mineralization.[14]

CO_2 mineralization can be categorized into direct and indirect mineralization based on reaction pathways.[15–17] While direct mineralization is thermodynamically favorable for spontaneous reactions, it has slow reaction kinetics, making it unsuitable for large-scale industrial processes. On the other hand, indirect mineralization involves two sequential processes: the extraction of Ca or Mg from minerals using various chemicals under acidic conditions, followed by the carbonization of the extracted Ca and Mg under alkaline conditions.[18–20] The indirect route is particularly intriguing due to its mild carbonation conditions, high carbonation efficiency, and production of pure products. The key to its large-scale industrial application lies in the selection of leaching agents.

Park and Fan[21] delved into the intricacies of the pH swing reaction phenomenon during CO_2 mineralization. This particular reaction bears a distinctive advantage in that it allows for the concurrent execution of mineral extraction and carbonation reactions under optimal pH conditions. Specifically, acidic conditions facilitate efficient mineral extraction, while basic conditions are conducive to the carbonation process. Ammonium chloride as a leaching agent can precisely change the pH of the solution spontaneously by extracting calcium ions and precipitating carbonates.[22,23] The reaction details are as follows:

Step 1 Calcium ions are extracted from the steel slag by reacting with an ammonium chloride solution. The acidity of the ammonium chloride solution enhances the extraction reaction of calcium ions.

$$4NH_4Cl\ (a) + 2CaO \cdot SiO_2\ (s) \rightarrow 2CaCl_2\ (a) + SiO_2\ (s) + 4NH_3\ (a) + 2H_2O\ (l).$$

Step 2 When CO_2 gas comes into contact with the extraction solution, $CaCO_3$ is produced, and the alkalinity of the solution enhances the absorption of CO_2. The NH_4Cl solution in the extraction solution of step 1 is regenerated with the precipitation of $CaCO_3$, and CO_2 is recovered as solid $CaCO_3$.

$$4NH_3\ (a) + 2CO_2\ (a) + 2CaCl_2\ (a) + 4H_2O\ (l) \rightarrow 2CaCO_3\ (s) + 4NH_4Cl\ (a)$$

Building upon the preceding analysis, this paper employs an ammonium chloride solution for the extraction of calcium elements from de-vanadiumized steel slag. The viability of the leaching reactions is elucidated through a thorough thermodynamic investigation, while leaching parameters undergo optimization *via* single-factor and response surface experiments. And study the reaction kinetics to determine the limiting link of the leaching reaction, to systematically look for further improvement schemes to improve the reaction rate and extraction efficiency to achieve the optimum.

II. EXPERIMENTAL

A. *Materials*

The steel slag used in this study is de-vanadiumized steel slag, provided by Chengde Iron and Steel Group Company Limited. The chemical composition of the vanadium slag and the de-vanadiumized steel slag was analyzed using X-ray fluorescence (XRF) as shown in Tables I and II, respectively. Examining the chemical makeup, it becomes evident that the predominant constituent in the vanadium slag is iron mineral, boasting 55.097 pct iron oxide and a mere 3.077 pct calcium oxide. ln stark contrast, the de-vanadiumized steel slag exhibits a significantly higher calcium oxide content at 60.37 pct, surpassing that of the vanadium slag. De-vanadiumized steel slag is more suitable as a raw material for CO_2 mineralization.

Table I. Analysis of Vanadium Slag Components

Name	Fe_2O_3	SiO_2	V_2O_5	Cr_2O_3	CaO	Al_2O_3	MgO	MnO
(Pct)	55.097	9.959	8.234	4.693	3.077	3.038	2.395	3.906

Table II. Analysis of De-vanadiumized Steel Slag Components

Name	CaO	Fe_2O_3	SiO_2	MgO	V_2O_5	P_2O_5	Al_2O_3	TiO_2
(Pct)	60.37	19.762	6.074	4.406	2.453	1.949	1.397	1.189

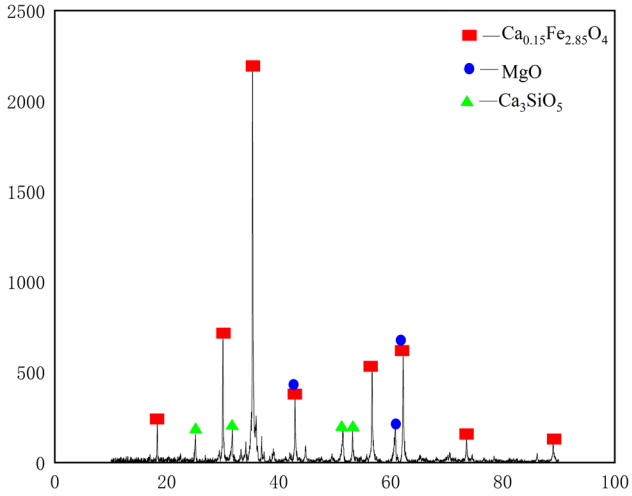

Fig. 1—XRD of vanadium slag.

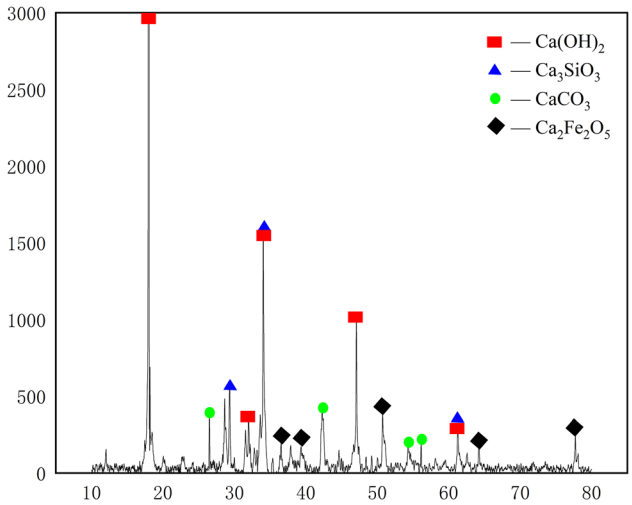

Fig. 2—XRD of de-vanadiumized steel slag.

XRD of vanadium slag and de-vanadiumized steel slag are shown in Figures 1 and 2, respectively. Figure 1 shows that the calcium-containing phase of vanadium slag is $Ca_{0.15}Fe_{2.85}O_4$ (calcium-iron oxide) and a small amount of Ca_3SiO_5 (tricalcium silicate). The main calcium-containing phase of devanadized steel slag is $Ca(OH)_2$. In addition, it also contains a small amount of Ca_3SiO_5 (tricalcium silicate), $Ca_2Fe_2O_5$ (calcium-iron oxide), and $CaCO_3$ (calcium carbonate).

This is because vanadium is extracted from vanadium slag using a magnetic separation followed by sodium roasting and then a wet leaching process.[24,25] Magnetic separation eliminates iron from the vanadium slag, and during high-temperature roasting in a rotary kiln or multi-hearth furnace, lime is introduced, leading to an elevation in the Ca element within the de-vanadiumized steel slag. The Ca element reacts with carbon dioxide decomposed by sodium carbonate to form $CaCO_3$, and then $Ca(OH)_2$ is finally formed by alkali leaching and precipitation. Notably, $Ca(OH)_2$ exhibits superior thermodynamic conditions compared to $Ca_{0.15}Fe_{2.85}O_4$. Therefore, in this study, de-vanadiumized steel slag was used as experimental raw material.

The de-vanadiumized steel slag was crushed using a ball mill to obtain different particle sizes. Then, the treated samples were sieved into four grades 10 mesh (1.7 mm), 50 mesh (0.27 mm), 100 mesh (0.15 mm), and 200 mesh (0.075 mm). Industrial-grade ammonium chloride chemicals were used.

B. *Experimental Procedure*

The leaching experiments on crushed de-vanadiumized steel slag were conducted in a temperature-controlled water bath. A 1 mol/L ammonium chloride solution was prepared by dissolving 10.7 g of ammonium chloride in 200 mL of distilled water in a beaker. The beaker was then placed in the water bath and heated until the thermometer measured the same temperature as the target temperature set for the experiment. A certain amount of de-vanadiumized steel slag was weighed and added to the reaction vessel. The beaker was sealed with plastic wrap to prevent the leaching solution from volatilizing during heating. The starting time of the leaching was recorded, and once finished, the de-vanadiumized steel slag and leachate were separated using filter paper. The concentration of metal ions in the leachate was measured using IRIS Intripedlls-$_2$ Plasma Emission Spectroscopy (ICP-AES).

The metal ion conversion ratio can be considered as the ratio of the total amount of metal ions leached from the leach solution to the total amount of metal elements in the de-vanadiumized steel slag. In addition, the total mass of metal ions in the leachate is equal to the concentration of metal ions in the leachate multiplied by the total volume of the leachate, and the concentration of metal ions in the leachate is equal to the concentration of metal ions detected by inductively coupled

plasma emission spectroscopy (ICP-AES) multiplied by the dilution factor. Therefore, the metal ion conversion rate can be expressed as

$$\eta_e = \frac{C_s^e \cdot V_s}{1000 \cdot W_s^e} \times 100 \text{ pct}, \quad [1]$$

$$W_s^e = W_s \times \omega_e \times \frac{M_e}{M_{E_xO_y}}, \quad [2]$$

$$C_s^e = C_I^e \times N, \quad [3]$$

$$e = \text{Ca}, \quad [4]$$

where η_e is the conversion rate of metal ions, pct; V_s is the liquid volume, L; W_s^e is the content of metal e in the de-vanadiumized steel slag, g; W_s is the mass of de-vanadiumized steel slag used for the test, g; C_s^e is the concentration of metal ion e in the leaching solution, mg/L; C_I^e is the concentration of metal ions detected by plasma emission spectrometry, mg/L; and N is the dilution multiple.

C. *Design of Experiments*

First, single-factor experiments were conducted by varying one of the four factors: temperature, time, particle size, and liquid–solid ratio.

The temperature (X_1, °C), time (X_2, min), particle size (X_3, mesh), and solid–liquid ratio (X_4, mL/g) were selected as variables in the post-experiment, and the calcium leaching rate was used as the response value, based on the Box–Behnken Design (BBD) method in the response surface methodology, a test plan with four factors and three levels was designed, and its coding values are shown in Table III. Table IV shows the design results of BBD.

A total of 30 groups of randomized trials were conducted, including six groups of center point repeated trials, which were used to evaluate test errors and data repeatability. The obtained experimental results can be fitted with the following quadratic polynomial model:[26]

$$y = \beta_0 + \sum_{i=1}^{4} \beta_i x_i + \sum_{i=1}^{4} \beta_{ij} x_i x_j + \sum_{i=1}^{4} \beta_{ii} x_i^2 + \varepsilon, \quad [5]$$

where y value is the dependent response variable (leaching rate of calcium); x_i is independent variables (temperature, time, particle size, liquid–solid ratio); β_0 is the model constant; β_i is the linear term coefficient; β_{ii} is the quadratic term coefficient; β_{ij} is the interaction term coefficient; and ε is the error term. The validity of the model can be determined by regression analysis (R^2) and analysis of variance (ANOVA, $p<0.05$). In the statistically significant model, the terms in the model were eliminated by backward elimination and the experimental data were redesigned to obtain the final model. The fitted polynomial equation can visually represent the relationship between the response variable and the independent variable with a surface plot.

Table III. Actual Values and Design Levels of the Variables

Independent Variables	Symbol	Coded Variable Levels		
		− 1	0	1
Temperature (°C)	X_1	25	50	75
Time (Minutes)	X_2	10	35	60
Particle Size (Mesh)	X_3	10	105	200
Liquid–Solid Ratio	X_4	8	54	100

*10 Mesh = 1.7 mm; 105 mesh = 0.14 mm; 200 mesh = 0.075 mm.

Table IV. Design for De-vanadiumized Steel Slag Leaching Experiment

Run	Independent Variables			
	X_1 (°C)	X_2 (Minutes)	X_3 (Mesh)	X_4
1	50	35	200	8
2	25	10	105	54
3	50	35	10	8
4	75	10	105	54
5	75	60	105	54
6	25	60	105	54
7	50	35	10	100
8	50	35	200	100
9	50	35	105	54
10	50	35	105	54
11	50	10	200	54
12	25	35	105	8
13	50	60	200	54
14	50	60	10	54
15	50	35	105	54
16	75	35	105	8
17	50	10	10	54
18	50	35	105	54
19	75	35	105	100
20	25	35	105	100
21	50	10	105	100
22	75	35	200	54
23	50	60	105	8
24	75	35	10	54
25	50	60	105	100
26	25	35	10	54
27	50	35	105	54
28	25	35	200	54
29	50	35	105	54
30	50	10	105	8

III. RESULTS AND DISCUSSION

A. *Thermodynamic Model of Calcium Ion Leaching from De-vanadiumized Steel Slag*

Following rigorous XRD analysis, the elemental composition of the de-vanadiumized steel slag manifests prominently as $Ca(OH)_2$ and $CaCO_3$.The ions in the leaching system include ammonium ions and chloride

ions, ammonium ions undergo hydrolysis to form ammonia monohydrate and hydrogen ions, ammonia monohydrate decomposes into ammonia gas and water, and the specific reactions are shown below:

$$NH_4^+ + H_2O \leftrightarrow NH_3 \cdot H_2O + H^+, \quad [6]$$

$$NH_3 \cdot H_2O = NH_3 + H_2O. \quad [7]$$

Calcium hydroxide and calcium carbonate cannot react directly with ammonium chloride spontaneously, the essence of the reaction is to react with the hydrogen ion ionized by ammonium ion. The specific reaction is as follows:

$$Ca(OH)_2 + NH_4Cl = CaCl_2 + NH_3 + 2H_2O, \quad [8]$$

$$CaCO_3 + NH_4Cl = CaCl_2 + NH_3 + CO_2 + H_2O. \quad [9]$$

Combining Eqs. [6] through [9] the reaction of the calcium-containing phase in the ammonium chloride solution occurs as follows:

$$Ca(OH)_2 + 2H^+ = Ca^{2+} + H_2O, \quad [10]$$

$$CaCO_3 + 2H^+ = Ca^{2+} + H_2O + CO_2. \quad [11]$$

Then, thermodynamic calculations were performed by FactSage software to calculate the Gibbs free energy of Reactions (10) and (11) as a function of the equilibrium constant and leaching temperature.

As can be seen from Figure 3, the standard Gibbs free energy of the reaction of $Ca(OH)_2$ and $CaCO_3$ in ammonium chloride solution is less than zero in the leaching temperature range, which indicates that both can react spontaneously with the ammonium chloride solution. This unequivocally signifies the inherent spontaneity of both reactions in the presence of the ammonium chloride solution. Furthermore, the graphical representation illuminates a discernible trend—the limit of the reaction involving the $CaCO_3$ phase and ammonium chloride solution experiences a decrement as the leaching temperature escalates. This phenomenon underscores the inhibitory impact exerted by elevated leaching temperatures on the leaching of calcium ions associated with the $CaCO_3$ phase. In stark contrast, the alteration in limits pertaining to the $Ca(OH)_2$ phase manifests a comparatively marginal shift, indicating a less pronounced effect of increased temperature on the leaching dynamics of $Ca(OH)_2$ phase.

1. *Model establishment*

In the leaching process of de-vanadiumized steel slag, the system is not simply a chemical reaction, but a multiphase system of multiple chemical reactions coupled in a parallel process. Therefore, the interaction between the reactions needs to be taken into account, and the total free energy is minimized when the system is in thermodynamic equilibrium. The chemical equilibrium problem of the leaching process can be transformed into a mathematical minimization problem with constraints.

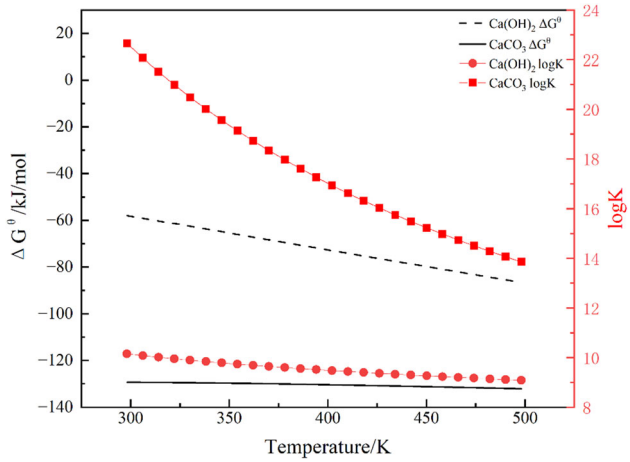

Fig. 3—Thermodynamic parameters *vs* temperature.

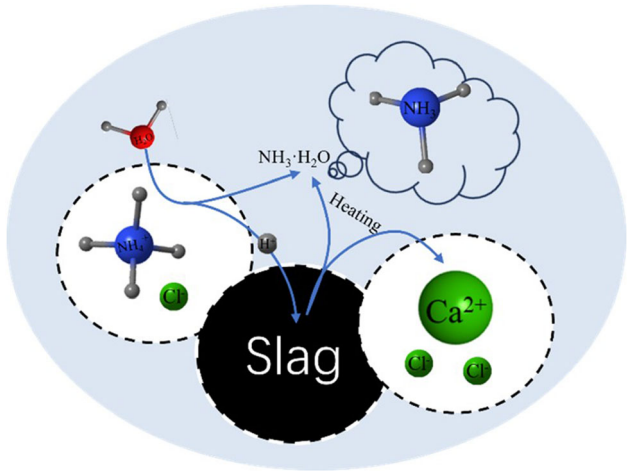

Fig. 4—Reaction mechanism of calcium ion leaching process.

Illustrating the leaching of calcium hydroxide and the calcium carbonate phase in an ammonium chloride solution, we establish a thermodynamic model elucidating the calcium ion leaching rate within this process. Assuming that the leaching of other metal ions in the leaching solution is very small and negligible, only calcium ions, ammonium chloride molecules, chloride ions, hydroxide ions, and ammonium ions are present in the system after leaching, the 1 pct solution is taken as the standard state for analysis, and the minimum free energy method is adopted. The intricate details of the calcium ion leaching process's reaction mechanism are visually depicted in Figure 4.

The calcium-containing phases in de-vanadiumized steel slag are calcium hydroxide [$Ca(OH)_2$] and calcium carbonate phase ($CaCO_3$); within the leaching system, set in an ammonium chloride solution with a concentration denoted as C_0, and accounting for the neglect of water ionization, the consumption of hydrogen ions is distributed proportionally in alignment with the standard Gibbs free energy of their individual reactions.

The leaching system is in a solution of ammonium chloride at a concentration of C_0, ignoring the ionization of water itself, while the proportion of hydrogen ions they consume is distributed in proportion to the standard Gibbs free energy of their respective reactions. For this reason, the main reactions that can occur during leaching are

$$Ca(OH)_2 + 2H^+ = Ca^{2+} + H_2O, \quad [12]$$

$$CaCO_3 + 2H^+ = Ca^{2+} + H_2O + CO_2. \quad [13]$$

Because ammonium chloride is a strong acid and weak base salt when dissolved in water, complete ionization occurs, and the ionized ammonium ions are hydrolyzed to produce hydrogen ions in the solution, so the ammonium chloride solution itself has a hydrolysis equilibrium of ammonium ions.

$$NH_4^+ = NH_3 + H^+. \quad [14]$$

Assume that the hydrolysis degree of (14) is α the equilibrium constant is K

$$\Delta G = -RT\ln K, \quad [15]$$

$$K = \frac{\alpha^2 \times C_0}{1-\alpha}. \quad [16]$$

The primary components of the leaching solution system at this time are calcium ions Ca^{2+}, ammonium ions NH^{4+}, hydrogen ions H^+, and chloride ions Cl^-. At this point, the leaching system is at its most stable, and its free energy is at its lowest. Furthermore, the impact of the leaching behavior of other metal ions in de-vanadiumized steel slag on calcium ions was disregarded and computed using a hypothetical 1 pct solution as the standard state due to the extremely low leaching rate of other metal ions in the slag.

Assume that when the slag leaching is stable, the mass percent of calcium ions in the leachate is $\omega_{Ca^{2+}}$,the mass percent of ammonium ions is $\omega_{NH_4^+}$, the mass percent of chloride ions is ω_{Cl^-}, the mass percent of hydrogen ions is ω_{H^+}, and the initial concentration of ammonia chloride is C_0, mol/L. Then, there is the objective function:

$$\min \Delta_m G = \sum_1^i x_i(\Delta G^O + RT\ln(K_i)). \quad [17]$$

Expanding Eq. [17] to obtain Eq. [18]:

$$\min \Delta_m G = x_1\Delta G^O + RT\ln\frac{\alpha_{Ca^{2+}}}{\alpha_{H^+}^2} + x_2\left(\Delta G^O + RT\ln\frac{\alpha_{Ca^{2+}}}{\alpha_{H^+}^2}\right). \quad [18]$$

Assuming that the molar concentration of calcium ions in the leached solution is very small and the solution is a dilute solution, the activity of the metal ions in the solution is calculated with the mass of 1 pct solution as the standard state, then there are

$$\alpha_{Ca^{2+}} = \omega_{Ca^{2+}}; \quad \alpha_{H^+} = \omega_{H^+}; \quad \alpha_{NH_4^+} = \omega_{NH_4^+}. \quad [19]$$

The constraints are

$$2\frac{\omega_{Ca^{2+}} \times m_0}{M_{Ca^{2+}}} + \frac{\omega_{NH_4^+} \times m_0}{M_{NH_4^+}} + \frac{\omega_{H^+} \times m_0}{M_{H^+}} = C_0, \quad [20]$$

$$x_1 = \xi_1 \times \frac{\omega_{Ca^{2+}} \times m_0}{M_{Ca^{2+}}}, \quad [21]$$

$$x_2 = \xi_2 \times \frac{\omega_{Ca^{2+}} \times m_0}{M_{Ca^{2+}}}, \quad [22]$$

$$\xi_1 = \frac{\Delta G^\theta_{Ca(OH)_2)}}{\Delta G^\theta_{Ca(OH)_2)} + \Delta G^\theta_{CaCO_3}}, \quad [23]$$

$$\xi_2 = \frac{\Delta G^\theta_{CaCO_3}}{\Delta G^\theta_{Ca(OH)_2)} + \Delta G^\theta_{CaCO_3}}, \quad [24]$$

$$2\frac{\omega_{Ca^{2+}} \times m_0}{M_{Ca^{2+}}} + \frac{\omega_{H^+} \times m_0}{M_{H^+}} + \alpha\frac{\omega_{NH_4^+} \times m_0}{M_{NH_4^+}} \le V \cdot C_0 \cdot \alpha, \quad [25]$$

$$\Delta G^\theta_{NH_4^+} + RT\ln\frac{\omega_{H^+}}{\omega_{NH_4^+}} \times \frac{m_0 \times M_{NH_4^+}}{M_{H^+}} \ge 0, \quad [26]$$

$$0 < \frac{\omega_{Ca^{2+}} \times m_0}{M_{Ca^{2+}}} \le \frac{w \times m_s}{M_{CaO}}, \quad [27]$$

$$\Delta G^\theta_{NH_4^+} = -RT\ln K, \quad [28]$$

$$K = \frac{\alpha^2 \times C_0}{1-\alpha}, \quad [29]$$

where ΔG represents the mixed Gibbs free energy in the reaction process of the leaching system, kJ/mol; $\Delta G^\theta_{NH_4^+}$ denotes the standard Gibbs free energy of the hydrolysis reaction of ammonium ion, kJ/mol; and denotes the free energy of the two reactions, kJ/mol; V denotes the volume of the leaching solution, ml; m_0 denotes the total mass of leached mixed slurry, g; m_s denotes the total mass of slag, g; R denotes the gas constant; T denotes leaching reaction temperature, K; denotes the percentage content of alkaline earth metals in the slag.

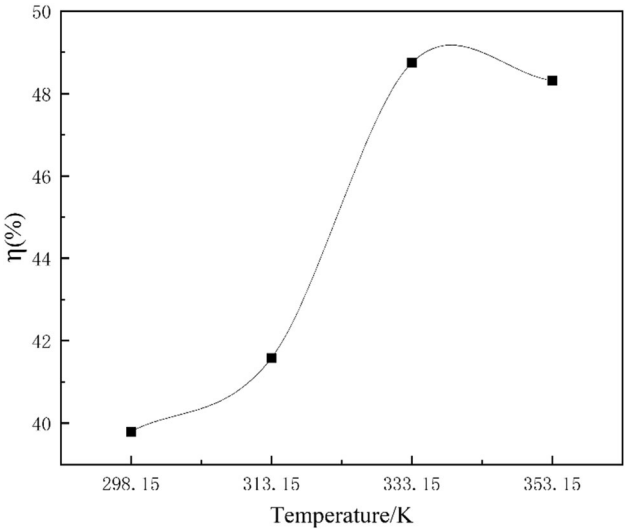

Fig. 5—Leaching rate of calcium ions as a function of leaching temperature.

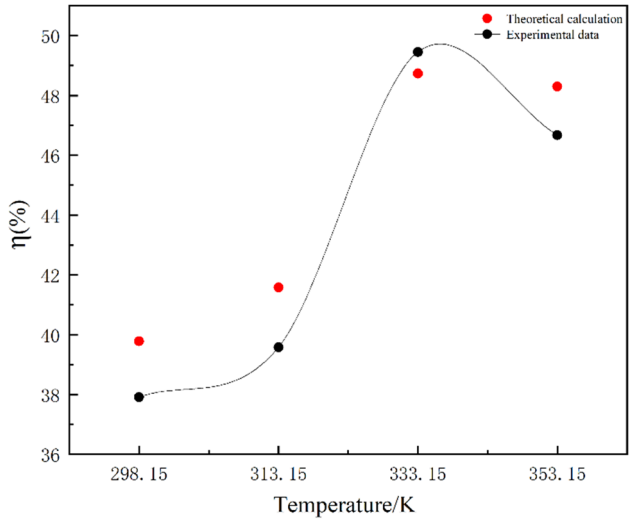

Fig. 6—Experimental and predicted values.

Where Eq. [20] indicates that the leaching solution maintains charge conservation and the solution system is electrically neutral, Eqs. [21] through [24] indicate that the hydrogen requirements of the two parallel reactions are assigned according to the standard Gibbs free energy of the leaching reaction; Eq. [25] indicates that the amount of hydrogen ions consumed to participate in the leaching reaction and the number of hydrogen ions required to maintain the equilibrium of ammonium ion hydrolysis is no more than the number of hydrogen ions for ammonium ion hydrolysis; Eq. [26] indicates that the ammonium ion is no longer hydrolyzed after the equilibrium of the leaching system; Eq. [27] indicates that the amount of calcium ions in the solution is no more than the total amount of calcium in the de-vanadiumized steel slag; Eq. [28] and [29] represent the functional relationship between the degree of hydrolysis of ammonium ions.

2. *Model solver*

The leaching rate of calcium ions in de-vanadiumized steel slag as a function of leaching temperature can be calculated by MATLAB software. The leaching rate of calcium ions as a function of leaching temperature for different temperature conditions is given in Figure 5.

From Figure 5, it can be seen that the leaching rate of alkaline earth metal ions in solution showed a pattern of increasing, then decreasing with the increase of leaching temperature in the leaching temperature range. When the concentration of ammonium chloride is 1 mol /L and leaching at 25 °C, the maximum leaching rate of the leaching solution at equilibrium is about 39.79 pct, the maximum leaching rate of alkaline earth metal ions was 41.58 pct when the leaching temperature was increased to 50 °C and the leaching process was balanced. When the temperature continued to increase to 60 °C, the leaching rate increased to the maximum value of 48.74 pct, and then decreased to 48.31 pct when the temperature was raised again.

Table V. Error Between Predicted and Experimental Values

Run	Temperature (°C)	Calculation	Experiment	Error (Pct)
1	25	39.79	37.2	4.93
2	40	41.58	39.59	5.02
3	60	48.74	49.45	1.44
4	80	48.31	46.68	3.49

3. *Model validation*

Next chapter's data from a single-factor influence experiment are mutually confirmed with the prediction model of the leaching rate of de-vanadiumized steel slag based on Gibbs' free energy minimal theory coupling to examine the prediction model's accuracy. Throughout the experiment, a solution containing 1 mol/L of ammonium chloride was utilized, and leaching temperatures ranged from 25 °C to 80 °C. (The reason for not discussing 100 °C is that water vapor is generated at 100 °C, and the reactions within the leachate at this point are different from those below 100 °C. The thermodynamic model is no longer appropriate for such reactions, which are described in detail in the next section.) The stirring intensity of the experiment was 400 r/min, and the liquid–solid ratio of the solution was 40 mL/g. The test results are shown in Figure 6.

As can be seen in Figure 6, it is evident that the calculated leaching rate of calcium ions, derived from the prediction model utilizing Gibbs free energy coupling for the calcium leaching rate of de-vanadiumized steel slag, aligns well with the experimental values. Detailed discrepancies between the predicted and actual values are provided in Table V, revealing errors that consistently remain below 10 pct in relative terms. This shows that the proposed prediction model for the leaching rate of calcium ions can respond well to the leaching process of de-vanadiumized steel slag in ammonium chloride solution.

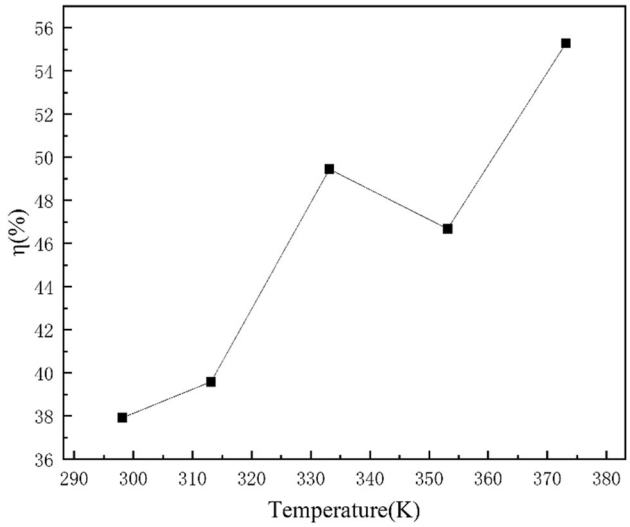

Fig. 7—Effect of temperature on leaching rate.

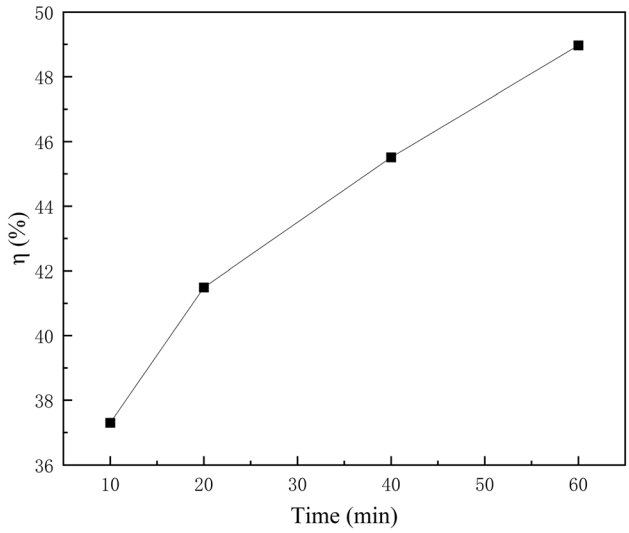

Fig. 8—Effect of time on leaching rate.

B. *The Influence of Temperature, Time, Particle Size, Liquid–Solid Ratio on the Calcium Ion Leach Rate*

First, the variation of leaching reaction conversion with reaction temperature was observed. Figure 7 illustrates the leaching rate of 0.075 mm de-vanadiumized steel slag at different temperatures over a 60-minute duration. Appropriately increasing the temperature can increase the leaching rate of calcium ions and improve the thermodynamic conditions of calcium ion leaching. With further increase in temperature, the solubility of calcium hydroxide decreases, resulting in a decrease in the leaching rate of Ca ions. Upon reaching the inflection point, the water initiates evaporation, giving rise to water vapor. This leads to an augmented contact between water vapor and steel slag, amplifying the reaction interface and facilitating the formation of free calcium. Consequently, the leaching rate experiences further enhancement as the temperature is raised during the latter part of the process. It can be seen from Figure 7 that the leaching rate is higher when the leaching temperature is 60 °C, so the subsequent experiments are all carried out at a temperature of 60 °C. Then, the effect of reaction time on the leaching rate was observed. In Figure 8, the curve of calcium leaching rate in de-vanadiumized steel slag showed an increasing trend with the increase in reaction time.

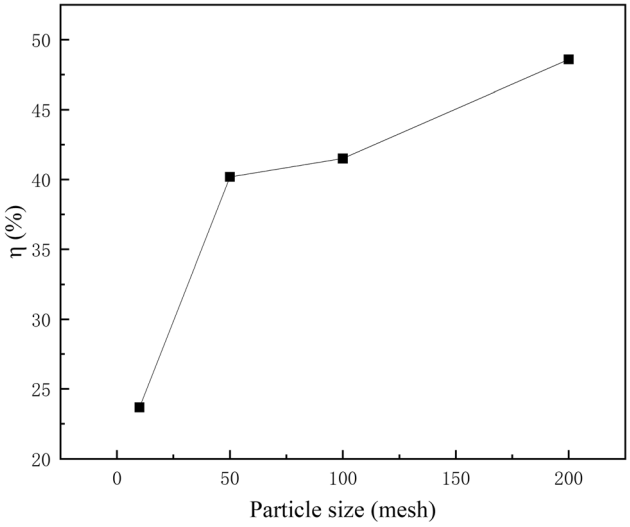

Fig. 9—Effect of particle size on leaching rate.

The particle size of the slag also has a significant effect on the conversion rate of the leaching reaction. Therefore, the leaching reaction was carried out for slag of different particle sizes. The conversion rate of the leaching reaction for each particle size is shown in Figure 9. As the particle size becomes smaller, the conversion rate increases and reaches the maximum conversion rate of 48.59 pct when the particle size of the de-vanadiumized steel slag is 0.075 mm. The relationship stems from the principle that a reduction in particle size corresponds to a heightened exposure of the mineral surface. As the specific surface area of the minerals increases, there is a maximized contact between the mineral and the leaching solution, resulting in a comprehensive interaction. In turn, expands the reaction area, thereby elevating the reaction rate and consequently augmenting the leaching rate. On the other hand, according to the study in Section III–F the diffusion process of calcium from the inside of the de-vanadiumized steel slag to the surface of the de-vanadiumized steel slag is one of the speed-controlling links. Therefore, the calcium ions generated inside the steel slag with large particles cannot diffuse into the solution in time, thus affecting the reaction rate.

As elucidated in Section III–F, the mass transfer process stands out as a speed-controlling factor in the leaching process, with the liquid–solid ratio exerting a significant influence on this process. To investigate this, leaching experiments were conducted at various liquid–solid ratios, and the results are depicted in Figure 10. It can be seen that the calcium leaching rate increases and then decreases with the increase of liquid–solid

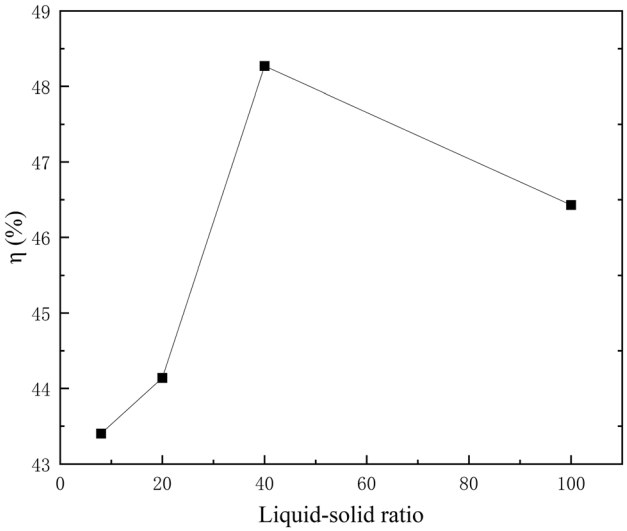

Fig. 10—Effect of liquid–solid ratio on leaching rate.

ratio. In the leaching system, a low liquid–solid ratio results in a higher pulp concentration. However, if the pulp concentration is too high, it can negatively impact the mass transfer and diffusion of the pulp, ultimately leading to a decrease in the leaching rate. Conversely, an excessively large liquid–solid ratio reduces the calcium concentration in the leaching solution, impacting calcium enrichment and resulting in a decline in the leaching rate.

Therefore, based on the single-factor analysis, the leaching process should be carried out under conditions of higher than 60 °C lower than 80 °C, time more than 60 minutes, raw material particle size more than 200 mesh, and liquid-solid ratio of 40.

C. *Regression Model and Analysis of the Significance of Response Surface*

The results of the second-order regression model analysis of variance (ANOVA) for leaching rate are shown in Table VI. The accuracy and variability of the model can be verified by determining the value of the coefficient R^2. Joglekar and May[27] argued that R^2 should be at least 0.80 to better fit the model; when R^2 is close to 1.0, it indicates that the actual values correlate well with the predicted values. It can be seen from Table VI, that the coefficient of determination (R^2 = 0.205) and the adjusted coefficient of determination (Adj. R^2 = 0.8650) are close to 1, which implies that the regression model is adequate. "Adeq.precision" represents the signal-to-noise ratio (SNR), and the value of 10.83 (> 4) indicates that the model can simulate the experiment well.[28]

The significance of the regression coefficients was estimated using *p*-values and *F*-values (Table VII). The ratio of the mean square to the residual ratio is the *F*-value. The *p*-value is used to check the significance of the coefficient. In general, a value of "probability > F" not exceeding 0.05 indicates that the model term is significant. If the magnitude of *F* is larger and the *p*-value is smaller, the corresponding variable becomes more significant. The model value of 10.76 and the *p*-value (< 0.0001) indicate that the model is highly significant for leaching rate.[29] Based on the *p*-value, X_3 has the most significant effect on the response.

Table VI. Analysis of Variance of Second-Order Regression Model for Leaching Rate

Source of Variation	Sum of Squares	Degree of Freedom	Mean Square	*F* Value	*p*-Value Probability > *F*
Residual	210.77	13	16.21		
Lack of Fit	198.26	10	19.83	4.76	0.1130
Pure Error	12.51	3	4.17		
Cor Total	2707.81	29			

*R^2 = 0.205; R^2(adj.) = 0.8650; Adeq. precision = 10.83 (> 4)

Figure 11 shows the relationship between the predicted and actual values. It can be seen that the correlation between the variables and the leaching rate can be well described by the empirical model, which provides evidence for the validity of the regression model. Based on these results, the prediction model is described as a second-order polynomial equation [30]:

$$\begin{aligned} Y = {} & 36.40 + 2.64 \times A + 1.67 \times B + 11_2 \times C \\ & + 4.50 \times D + 2.33 \times A \times B + 0.073 \times A \times C \\ & - 0.27 \times A \times D - 1.95 \times B \times C - 0.60 \times B \\ & \times D - 0.10 \times C \times D + 0.90 \times A^2 - 0.94 \times B^2 \\ & - 6.63 \times C^2 - 2.10 \times D^2. \end{aligned} \quad [30]$$

Figure 12 shows the relationship between residual plots and normal probability for leaching rate. The extreme points of the normal probability plot of residuals are − 2.212 and + 2.361, proving the errors are normally distributed and nonsignificant. The approximately straight fitting line indicates that the variance of the original experiment is a constant for all values of *Y*. Therefore, the empirical model is suitable for describing the leaching rate of calcium from de-vanadiumized steel slag.

D. *Effect of Process Variables*

3D response surface and contour plots of the leaching rate of de-vanadiumized steel slag show the effect of independent variables on the dependent variable.

In Figures 13(a) and (b), the impact of the interaction factor between temperature and particle size is illustrated under the conditions of a liquid–solid ratio of 54 and a time span of 50 minutes. Among them, Figure 13(b) is the projection of Figure 13(a) on the bottom surface. As the particle size diminishes, the specific surface area of the de-vanadiumized steel slag expands, resulting in an augmented leaching rate. However, the influence of leaching time on the leaching rate was not

Table VII. Regression Model of the Relationship Between Variables and Independent Variables

Source	Coefficient Estimate	Sum of Squares	DF	Mean Square	*F* Value	*p*-Value
Model		2441.91	14	174.42	10.76	< 0.0001
Intercept	36.40		1			
A-X_1	2.64	83.37	1	83.37	5.14	0.0410
B-X_2	1.67	33.40	1	33.40	2.06	0.1748
C-X_3	11.2	1705.04	1	1705.04	105.16	< 0.0001
D-X_4	4.50	242.73	1	242.73	14.97	0.0019
AB	2.33	21.62	1	21.62	1.33	0.2689
AC	0.073	0.021	1	0.021	1.297E^{-003}	0.9718
AD	− 0.27	0.30	1	0.30	0.019	0.8934
BC	− 1.95	15.25	1	15.25	0.94	0.0498
BD	− 0.60	1.45	1	1.45	0.090	0.7695
CD	− 0.10	0.040	1	0.040	2.467E^{-003}	0.9611
A^2	0.90	5.59	1	5.59	0.34	0.5673
B^2	− 0.94	6.11	1	6.11	0.38	0.5500
C^2	− 6.63	301.08	1	301.08	18.57	0.0008
D^2	− 2.10	30.24	1	30.24	1.87	0.1952

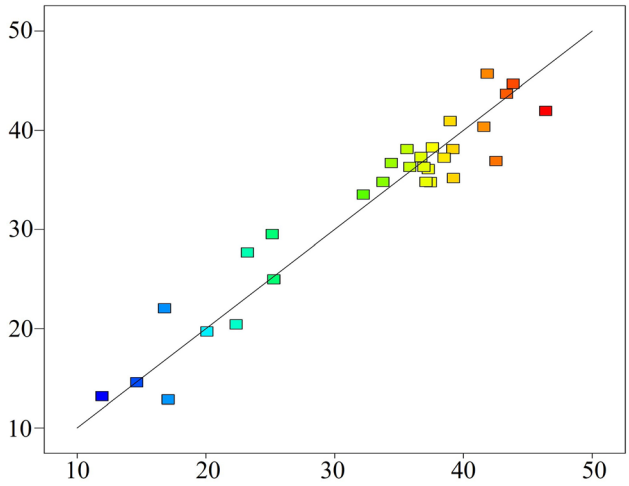

Fig. 11—Predicted and true values.

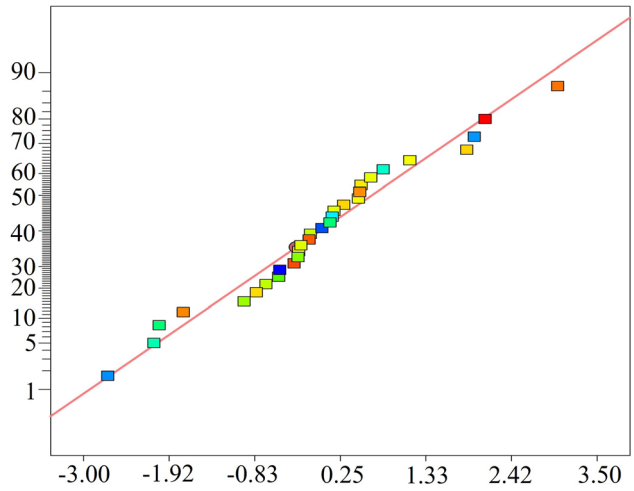

Fig. 12—Residual plots of normal probability for leaching rate.

significant. According to the *F*-value and *p*-value (Table VII), the interaction of particle size was significant compared to leaching time. Based on ANOVA (Table VII), the interaction effect of temperature and particle size was negligible (*p*-value = 0.9718).

The impact of temperature and particle size on the leaching rate at 50 °C and a liquid–solid ratio of 54 is depicted in Figures 14(a) and (b). Among them, Figure 14(b) is the projection of Figure 14(a) on the bottom surface. The second-order influence of particle size and time is clearly visible in the figure. It is evident that the leaching rate rises over time and does so within the confines of a comparatively flat curve. The impact of the interaction between particle size and time on the leaching rate was determined to be significant, as indicated by the ANOVA analysis in Table VII.

Figure 15(a) and (b) presents the interaction between particle size and liquid–solid ratio on the leaching rate, conducted at a temperature of 50 °C with 30 minutes of stirring. Among them, Figure 15(b) is the projection of Figure 15(a) on the bottom surface. The leaching rate increased with the increase of mesh and liquid–solid ratio. This may be due to the increase in liquid–solid ratio which leads to a smaller slurry concentration, each particle can be fully combined with the solution, increasing the reaction area and mass transfer rate. Simultaneously, a smaller particle size translates to a larger specific surface area, further enhancing the reaction area and facilitating mass transfer. It is also clear from the value of *F* in Table VII that the interaction between particle size and liquid–solid ratio also has a significant effect on the leaching rate.

E. *Parameter Optimization and Validation*

Based on the characteristics of contour lines and three-dimensional response surfaces, it can be found that the significance of each factor to the test results is X_3 (particle size) > X_4 (liquid–solid ratio) > X_1 (temperature) > X_2 (time), and the interaction between the factors X_2X_3 and X_3X_4 is significant.

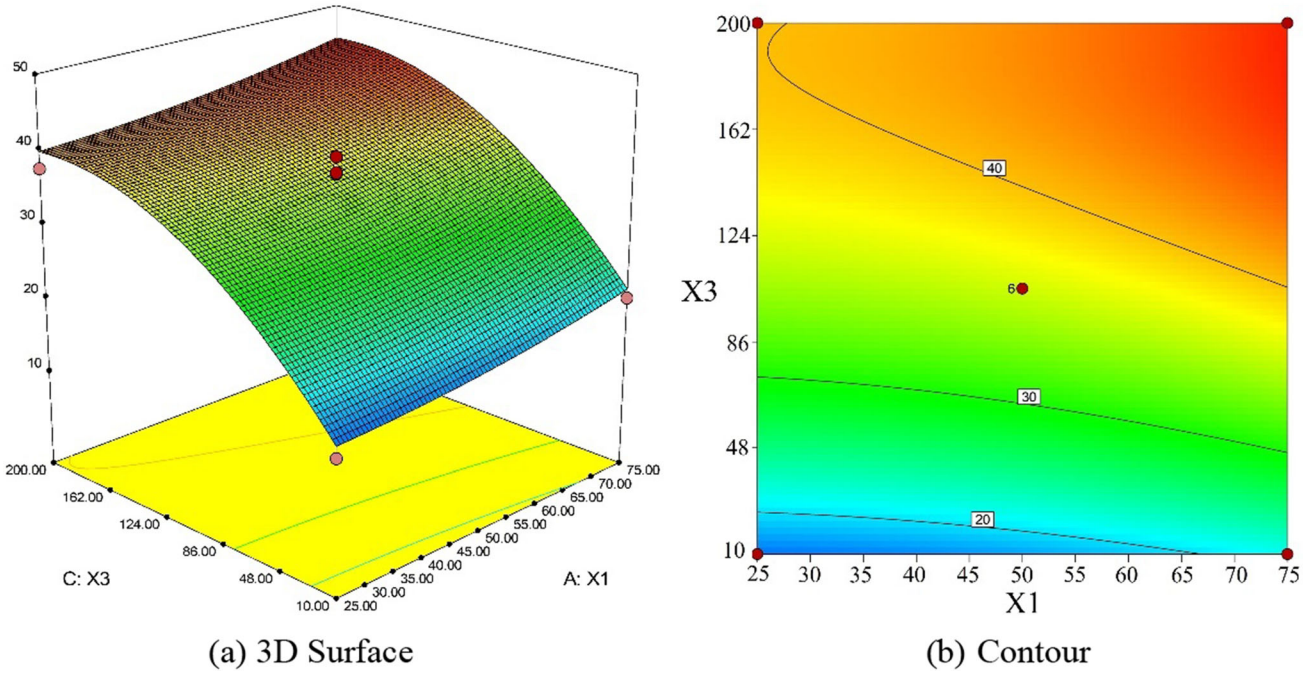

Fig. 13—Effect of temperature and particle size on leaching rate.

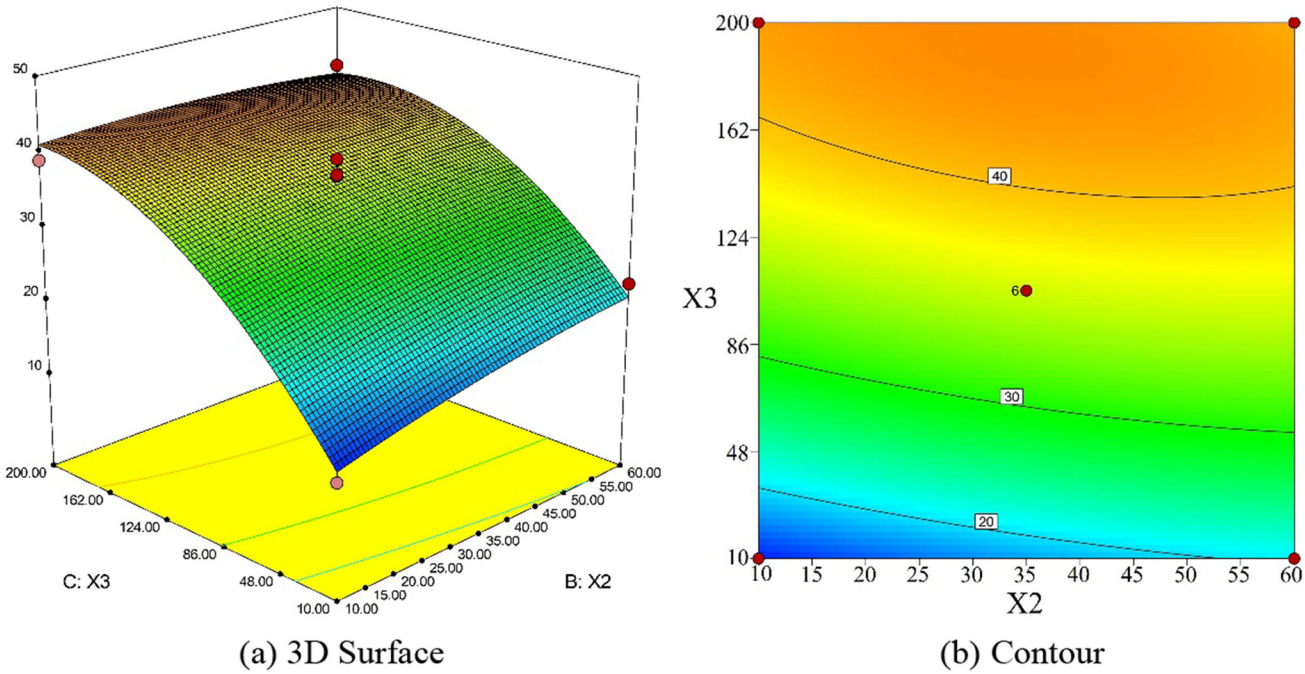

Fig. 14—Effect of time and particle size on leaching rate.

Utilizing response surface design and optimization, the optimization parameters are temperature is 80 °C, time is 69.85 minutes, particle size is 0.09 mm, and liquid–solid ratio is 89.74, taking into account the maximum leaching rate of the de-vanadiumized steel slag. The three replication trials had leaching rates of 50.26, 48.73, and 51.67 pct under ideal conditions, with an average of 50.22 pct; the variation from the expected value of 49.76 pct was only 0.2 pct. To sum up, the model can accurately forecast when calcium ions will leach from de-vanadiumized steel slag. The process parameters of the calcium leaching element of the

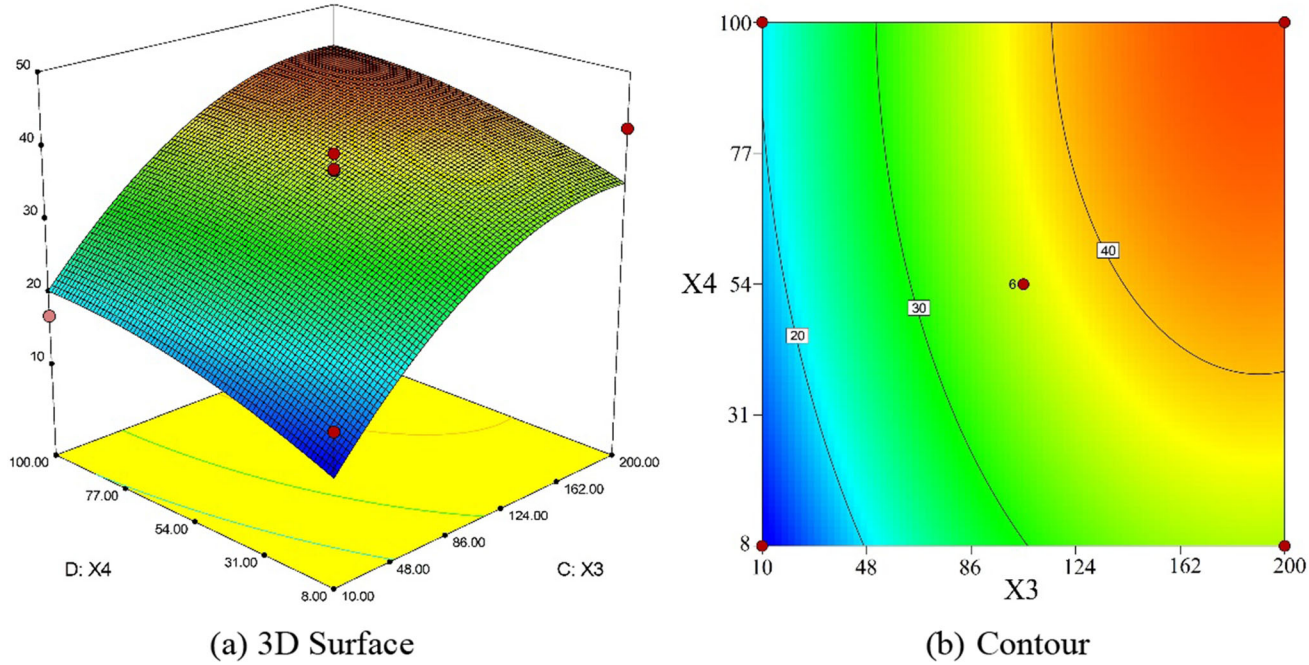

Fig. 15—Effect of particle size and liquid-to-solid ratio on leaching rate.

de-vanadium steel slag are therefore correct and acceptable based on RSM, offering a trustworthy theoretical foundation for industrial production.

F. *Kinetic Analysis of Calcium Leaching from De-vanadiumized Steel Slag*

1. *Determination of the reaction rate*

To ascertain the leaching rate parameters of de-vanadiumized steel slag in an ammonium chloride solution, 5 g of the slag was subjected to experiments at temperatures of 25 °C, 40 °C, 60 °C, and 80 °C. Varied leaching times were employed to discern the relationship between the conversion rate of calcium ions and leaching duration. The experiments were conducted under constant stirring at a rate of 400r/min within a temperature-controlled water bath, and the test results are shown in Figure 16.

From the leaching curve, it can be seen that the conversion rate of calcium ions decreases gradually with the increase of leaching time and finally stabilizes. At the beginning of the leaching of de-vanadiumized steel slag in ammonium chloride, the reaction rate is fast, but soon the conversion rate decreases and shows a certain self-blocking phenomenon. Therefore, the leaching process of de-vanadiumized steel slag in ammonium chloride can be better described by using Drozdov equation with a self-rejection factor.

$$\frac{1}{t}\ln\frac{1}{1-x}-\beta\frac{x}{t}=k_{\mathrm{m}}, \qquad [31]$$

where t is the leaching time, h; x is the calcium ion conversion rate, pct; β is the self-rejection facto; and k_{m} is the reaction rate constant.

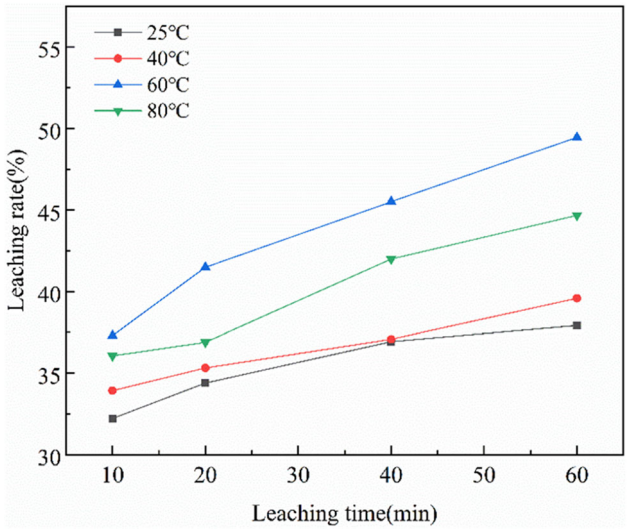

Fig. 16—Relationship between time and leaching rate at different temperatures.

From the Drozdov equation, it follows the relationship between $\frac{1}{t}\ln\frac{1}{1-x}$ and $\frac{x}{t}$, the slope of the curve is the self-rejection factor, and the curve intercept is the rate constant of the leaching reaction of de-vanadiumized steel slag in ammonium chloride. According to the test data, a scatter plot is made, and Figure 17 and Table VIII can be obtained through linear fitting. It can be clearly seen from Figure 17 and Table VIII that the reaction rate constant of the leaching process of de-vanadiumized steel slag in ammonium chloride increases with the increase in temperature.

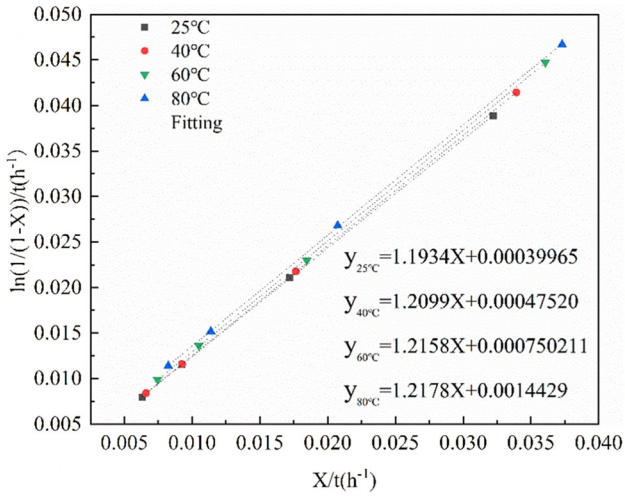

Fig. 17—Relationship between $\frac{1}{t}\ln\frac{1}{1-x}$ and $\frac{x}{t}$.

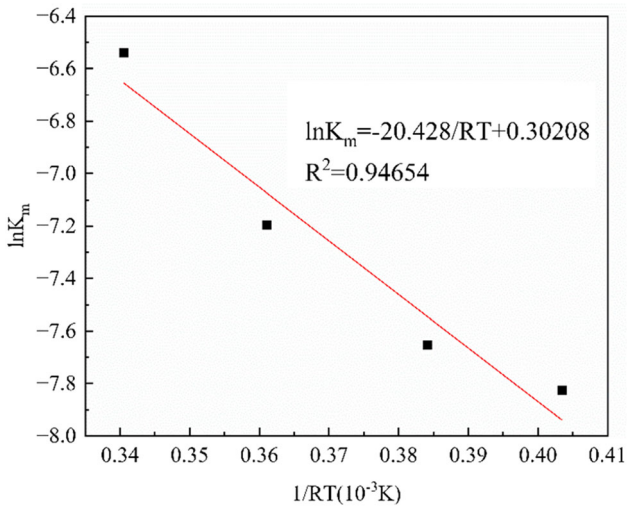

Fig. 18—Plot of $\ln K_m$ *vs* $1/T$.

Table VIII. Experimental Fitting Data of Ca^{2+}

Element	Temperature (°C)	Reaction Rate Constant	Self-Rejection Factor	Degree of Fit
Ca^{2+}	25	0.0003997	1.1934	0.99996
	40	0.0004752	1.2099	0.99999
	60	0.0007502	1.2158	0.9992
	80	0.0014443	1.2178	0.99989

2. *Calculation of activation energy of reactions*

Based on the reaction rate constants obtained in the previous section, the apparent activation energy of the leaching reaction can be found by linearly fitting $\ln K_m$ and $1/T$ using the Arrhenius equation[30]

$$\ln K_m = \ln A - \frac{E_a}{RT}, \qquad [32]$$

where K_m is the reaction rate constant; A is the frequency factor; E_a is the apparent activation energy, kJ/mol; R is the gas constant, 8.314 J/(mol·K); and T is the leaching temperature, K.

The curve of calcium ion conversion $\ln K_m$ *vs* $1/T$ is shown in Figure 18, the degree of fit of the curve was $R^2 = 0.94625$, and the fit was good. The calculation shows that the apparent activation energy of the leaching reaction is 20.428 kJ/mol, and the frequency factor is equal to 1.3527, the size of the activation energy represents the speed of the chemical reaction rate, the greater the activation energy, the more difficult the chemical reaction is, and the smaller the reaction rate is; on the contrary, the smaller the activation energy, the greater the reaction rate. Therefore, the activation energy can be used as an important indicator to judge the control step of multiphase reaction. In general, the activation energy of diffusion control is less than 13 kJ/mol, the activation energy of interface chemical reaction control is generally greater than 40 kJ/mol, and the activation energy of mixing control is 20 to 35 kJ/mol.[31] From the analysis of the activation energy of the leaching reaction, it can be seen that the leaching reaction of calcium ions from the de-vanadiumized steel slag in sodium chloride solution is controlled by the liquid-solid interface chemical reaction and diffusion mixing.

IV. CONCLUSIONS

This paper investigates the behavior of calcium leaching from de-vanadiumized steel slag in sodium chloride solution.

(1) When the calcium phase in the de-vanadiumized steel slag is leached in ammonium chloride, it cannot react directly but reacts with hydrogen ions produced by hydrolysis of ammonium ions.

(2) The thermodynamic model effectively characterizes the leaching process of de-vanadiumized steel slag in ammonium chloride solution. It accurately delineates the relationship between calcium ion leaching rate and reaction temperature, with a relative error below 10 pct when comparing predicted and experimental values.

(3) The leaching rate increases first and then decreases and then increases with the increase in temperature. Time and particle size were positively correlated with leaching rate. The effect of liquid–solid ratio on the leaching rate increases first and then decreases. The influence order of each parameter on the leaching rate of calcium ion is X_3 (particle size) > X_4 (liquid–solid ratio) > X_1 (temperature) > X_2 (time), and the interaction between X_2X_3 and X_3X_4 is significant. The optimum experimental conditions were as follows: temperature is 80 °C, time is 69.85 minutes, particle size is 0.09 mm, liquid–solid ratio is 89.74, and the maximum leaching rate of calcium ion was 49.76 pct.

(4) The self-resistance coefficient of the dynamic model increases in the range of 1.15 to 1.25. At the same time, the apparent activation energy of the leaching process is 20.428 kJ/mol, and the rate control step in the leaching process is the liquid–solid interface chemical reaction and diffusion step.

The next step will focus on improving the speed of the limiting link and the carbonation behavior of the leachate as well as on the high value application of the leach sludge to provide theoretical guidance for faster industrialization.

ACKNOWLEDGMENTS

The authors acknowledge the financial support for the National Natural Science Foundation (No. 52274316), the National Key R&D Program of China (No. 2022YFE0208100), the Anhui Provincial Key Research and Development Plan (202210700037), and the Xinjiang Autonomous Region Major Science and Technology Special (2022A01003-1).

CONFLICT OF INTEREST

The authors declare that they have no known competing financial interests or personal relationships that could have appeared to influence the work reported in this paper. The authors declare the following financial interests/personal relationships which may be considered as potential competing interests.

REFERENCES

1. H. Dang, R. Xu, J. Zhang, M. Wang, and J. Li: *Int. J. Miner. Metall. Mater.*, 2023.
2. IEA: *Global Energy Review 2021*, IEA, Paris, 2021.
3. B. Metz, O. Davidson, H. Coninck, M. Loos and L. Meyer: IPCC Special Report on Carbon Dioxide Capture and Storage. Prepared by Working Group III of the Intergovernmental Panel on Climate Change. Cambridge University Press, Cambridge, 2005, pp. 1–431.
4. M.N. Anwar, A. Fayyaz, N. Sohail, M.F. Khokhar, M. Baqar, W.D. Khan, K. Rasool, M. Rehan, and A. Nizami: *J. Environ. Manag.*, 2018, vol. 226, pp. 131–44.
5. M. Bai, Z. Zhang, and X. Fu: *Renew. Sustain. Energy Rev.*, 2016, vol. 59, pp. 920–26.
6. S. Park: *Energy*, 2018, vol. 153, pp. 413–21.
7. J.S. Lee and E.C. Choi: *Renew. Sustain. Energy Rev.*, 2018, vol. 93, pp. 753–58.
8. S. Pandey, V.C. Srivastava, and V. Kumar: *Can. J. Chem. Eng.*, 2021, vol. 99, pp. 467–78.
9. X. Xu, W. Liu, G. Chu, G. Zhang, D. Luo, H. Yue, B. Liang, and C. Li: *Hydrometallurgy*, 2019, vol. 184, pp. 151–61.
10. S. Yadav and A. Mehra: *J. CO2 Util.*, 2019, vol. 31, pp. 181–91.
11. M.H. Ibrahim, M.H. El-Naas, R. Zevenhoven, and S.A. Al-Sobhi: *Int. J. Greenh. Gas Control*, 2019, vol. 91, p. 102819.
12. Q. Zhao, X. Chu, X. Mei, Q. Meng, J. Li, C. Liu, H. Saxen, and R. Zevenhoven: *Front. Chem.*, 2020, vol. 8, p. 856.
13. USGS: *Mineral Commodity Summaries 2021*, USGS, Reston, 2021.
14. S.Y. Pan, Y.H. Chen, L.S. Fan, H. Kim, X. Gao, T.C. Ling, P.C. Chiang, S.L. Pei, and G. Gu: *Nat. Sustain.*, 2020, vol. 3, pp. 399–405.
15. K.D. Crom, Y.W. Chiang, T.V. Gerven, and R.M. Santos: *Chem. Eng. Res. Des.*, 2015, vol. 104, pp. 180–90.
16. S. Lee, J. Kim, S. Chae, J. Bang, and S.W. Lee: *J. CO2 Util.*, 2016, vol. 16, pp. 336–45.
17. W. Liu, L. Teng, S. Rohani, Z. Qin, B. Zhao, C.C. Xu, S. Ren, Q. Liu, and B. Liang: *Chem. Eng. J.*, 2021, vol. 416, p. 129093.
18. S. Teir, R. Kuusik, C. Fogelholm, and R. Zevenhoven: *Int. J. Miner. Process.*, 2007, vol. 85, pp. 1–15.
19. X. Dong: *Steelmaking*, 2008, vol. 24, p. 29.
20. J.M. Song: *Environ. Eng.*, 2010, vol. 28, p. 214.
21. P. Aha and L.S. Fan: *Chem. Eng. Sci.*, 2004, vol. 59, pp. 5241–47.
22. S. Kodama, T. Nishimoto, N. Yamamoto, K. Yogo, and K. Yamada: *Energy*, 2008, vol. 33, pp. 776–84.
23. Y. Sun, M.S. Yao, J.P. Zhang, and G. Yang: *Chem. Eng. J.*, 2011, vol. 173, pp. 437–45.
24. F. Gao, H. Du, S. Wang, B. Chen, J. Li, Y. Zhang, M. Li, B. Liu, and A.U. Olayiwola: *Miner. Process. Extr. Metall. Rev.*, 2023, vol. 44, pp. 352–64.
25. S. Zhang, G. Li, R. Xiao, J. Luo, L. Yi, and M. Rao: *J. Mater. Res. Technol.*, 2021, vol. 15, pp. 5712–22.
26. M. Bezerra, R. Santelli, E.P. Oliveira, L.S. Villar, and L.A. Escaleira: *Talanta*, 2008, vol. 76, pp. 965–77.
27. A. Joglekar and A. May: *Cereal Foods World*, 1987, vol. 32, pp. 857–68.
28. G. Lin, T. Hu, J. Peng, S. Yin, L. Zhang, W. Guo, and Y. Liu: *Arab. J. Sci. Eng.*, 2016, vol. 41, pp. 569–76.
29. Z.R. Zhang, S.H. Luo, J.C. Wang, M. Sun, S. Yan, Q. Wang, Y. Zhang, X. Liu, and X. Lei: *J. Energy Storage*, 2022, vol. 56, p. 105913.
30. X.W. Huang: *J. Capital Normal Univ. (Nat. Sci. Ed.)*, 1995, vol. 01, pp. 62–65.
31. H.X. Jin, J.Q. Li, and F.Z. Wu: *Chin. J. Eng.*, 2011, vol. 33, pp. 1071–78.